Ultraviolet resonance Raman and absorption difference spectroscopy of myoglobins: titration behavior of individual tyrosine residues

ARTICLE *in* BIOCHEMISTRY · JULY 1991

Impact Factor: 3.02 · DOI: 10.1021/bi00238a019 · Source: PubMed

3 AUTHORS, INCLUDING:

Sanford A Asher
University of Pittsburgh
312 PUBLICATIONS **13,115** CITATIONS
SEE PROFILE

Peter J Larkin
CYTEC Industries
6 PUBLICATIONS **73** CITATIONS
SEE PROFILE

Ultraviolet Resonance Raman and Absorption Difference Spectroscopy of Myoglobins: Titration Behavior of Individual Tyrosine Residues†

Sanford A. Asher,* Peter J. Larkin, and Junji Teraoka‡
Department of Chemistry, University of Pittsburgh, Pittsburgh, Pennsylvania 15260
Received February 5, 1991

ABSTRACT: The UV resonance Raman spectra of horse and sperm whale myoglobin excited at 240 nm show bands between 600 and 1700 cm^{-1} which derive from tyrosyl and tryptophyl residues. No significant contribution from phenylalanine and peptide backbone vibrations occurs at this excitation wavelength. We examine the pH dependence of the UV resonance Raman and UV absorption difference spectra of these myoglobins to correlate the local protein environment of the tyrosyl residues as given by the protein crystal structure to their pK_a values, molar absorptivities, and Raman cross sections. Some of our pK_a values for the tyrosinate residues of horse Mb differ from those of previous studies. We show that the λ_{max} values, the molar absorptivities, and the Raman cross sections are sensitive to the local environment of the tyrosinate residues in the protein. We relate differences in the tyrosyl absorption spectra to differences in Raman cross sections. In addition, we discuss the importance to the Raman cross sections of the local electromagnetic field enhancement due to the dielectric environment of the tyrosinate residues in the protein. This local field should scale the Raman cross sections in a way useful as a probe of the average aromatic amino acid residue environment.

UV resonance Raman spectroscopy has recently emerged as a promising new technique for the study of biomolecular structure and function (Asher, 1988; Su et al., 1989; Kaminaka et al., 1990; Hildebrandt et al., 1988; Harada & Takeuchi, 1986; Rava & Spiro, 1985; Copeland & Spiro, 1985a,b; Asher et al., 1983; Hudson & Mayne, 1984). While a few laboratories have begun to use this technique for protein structural studies, the major efforts up until now have centered on establishing the fundamental background information crucial for correctly interpreting future protein structural studies. The necessary model compound studies such as measurements of the aromatic amino acid cross sections (Sweeney & Asher, 1990; Ludwig & Asher, 1988; Asher et al., 1986; Rava & Spiro, 1984, 1985a; Johnson et al., 1986) and peptide amide Raman cross sections (Dudik et al., 1985a; Song & Asher, 1989; Krimm et al., 1989; Song et al., 1990; Copeland & Spiro, 1986, 1987; Caswell & Spiro, 1987; Mayne et al., 1985; Mayne & Hudson, 1987) are now complete as are studies of small peptides and small proteins. Furthermore, we have completed the necessary detailed photochemical Raman spectroscopic studies required to establish the experimental conditions over which pulsed laser UV Raman studies are immune from photophysics, photochemistry, and interference from excited-state intermediates (Johnson et al., 1986; Jones et al., 1987; Ludwig & Asher, 1988a; Teraoka et al., 1990; Harmon et al., 1990). Thus, the fundamental framework now exists to begin incisive studies of protein structure and function.

In the present study, we have utilized UV resonance Raman spectroscopy to examine the titration behavior of the tyrosine residues of horse and sperm whale myoglobin with the objective of determining the evolution of the environment of these residues as the protein unfolds under high pH conditions. Our study illustrates the dependence of tyrosine pK_a values upon local environment and examines the changes in environment of tyrosinates as the heme titrates and as the globin protein structure evolves as amino acid residues titrate due to pH increases. Some of our results agree closely with previous myoglobin titration studies (Hermans, 1962; Wilbur & Allerhand, 1976; Uyeda & Peisach, 1981; Hirsch & Peisach, 1986). However, our horse myoglobin pK_a values differ significantly from those of Uyeda and Peisach (1981).

In addition to conveying new information on myoglobin structure, this study demonstrates the sensitivity of the UV Raman cross sections to protein environment. Thus, the present study is important because it will serve as a central framework for future quantitative studies of tyrosinate environments in proteins.

Experimental Procedures

Lyophilized horse myoglobin (type I, from equine skeletal muscle) and sperm whale myoglobin were obtained from Sigma Chemical and U.S. Biochemicals Co., respectively. Although we did not further purify the protein (Hapner et al., 1986), this should not impact the comparison between our myoglobin pK_a values and those of Uyeda and Peisach (1981), for example. Uyeda and Peisach (1981) previously demonstrated that the dominant fractions IV and IIIb which account for 78% and 18% of the protein both have three tyrosines with essentially identical pK_a values. In fact, they show that a commercially available mixture gives identical pK_a results with those of the isolated fractions.

We prepared unbuffered stock solutions by dissolving the protein in deionized, purified water and added sodium perchlorate as the Raman internal intensity standard. The water was purified by using a four-stage Barnstead Nanopure ion-exchange system. The buffered myoglobin sample solutions at various pH values were prepared by diluting the appropriate volume of stock solution into phosphate or carbonate buffer. The final buffer and sodium perchlorate concentrations were 0.30 and 250 mM, respectively. Published molar absorptivities for aquomet sperm whale and horse myoglobins (Antonini & Brunori, 1971) were used to determine protein concentrations. A Perkin Elmer Lambda 9 UV-vis spectrophotometer was used to measure UV absorption difference spectra.

† This work was supported by NIH Grant IR01GM30741-09.
* Author to whom correspondence should be addressed.
‡ Present address: Osaka City University, Osaka, Japan.

0006-2960/91/0430-5944$02.50/0

The UV Raman spectrometer has been previously described (Asher et al., 1983; Jones et al., 1987). The 308-nm fundamental of a 200-Hz Lambda-Physik Model EMG 103 MSC XeCl excimer laser is employed to pump a Lambda-Physik Model FL 3002 dye laser, which is frequency-doubled to generate the UV excitation used in this study. The 0.175 mM protein solutions and the aromatic amino acid solutions (0.6 mM Tyr, 0.4 mM Trp, and 1.2 mM Phe) were recirculated through a 1.0-mm i.d. Suprasil quartz capillary by a peristaltic pump. The sampling optics used a 135° back-scattering geometry. The Raman scattered light was focused onto the entrance slit of a Spex Triplemate monochromator by an ellipsoidal mirror to avoid chromatic aberrations. The 1200 groove/mm grating used in the spectrograph stage of the Triplemate gave a spectral bandpass of 26 cm^{-1} at 240 nm for the spectrograph slit width of 200 μm. The polarization of the scattered light was randomized by a crystalline quartz wedge to avoid intensity artifacts deriving from any polarization efficiency bias of the monochromator. The scattered light was detected with a Princeton Applied Research OMA II system which utilizes a Model 1420 blue-enhanced intensified Reticon detector.

The sample solutions (10 mL) were irradiated for 5 min using pulse energy fluxes of ca. 0.5 mJ/cm^2 per pulse (total average power = 2.5 mW) and pulse repetition rates of 200 Hz. The Raman cross sections derive from measured peak height ratios between the tyrosinate band and that of the perchlorate internal standard, using the previously measured perchlorate cross sections (Dudik et al., 1985b). The sample pH values and absorption spectra were measured before and after the Raman spectral measurements to ensure that no irreversible photochemistry occurred during laser irradiation. The power flux dependence of the spectra was measured to ensure that the excitation flux densities used avoided saturation and photochemistry. Raman difference spectra used to monitor the tyrosinate concentrations were obtained by direct numerical subtraction of the spectra at various pH values from that at neutral pH.

The high-pH Raman and absorption difference spectra were measured immediately after preparation of the solutions. This was required in order to obtain reproducible high-pH absorption and Raman spectra due to observed time-dependent alterations in the protein structure; above pH 13.0, the 240-nm absorbance increases with time, presumably because of protein unfolding that leads to a decreased pK_a value for previously buried tyrosines. The high-pH stability depends upon solution conditions.

We recently demonstrated that >0.1 M ClO_4 concentrations affect the quaternary and tertiary structure of hemoglobin–ligand complexes (Song & Asher, 1991). As a result, we now advocate use of cacodylate and SeO_4 as UV Raman internal standards. For horse Mb, we observe that ClO_4^- decreases the high-pH stability. For example, a ca. 10% increase in $\Delta\epsilon_{240}$ occurs within 10 min for horse myoglobin at pH 13.05 in the presence of 0.25 M $NaClO_4$. In contrast, at 0.25 M KCl, a similar ca. 10% $\Delta\epsilon_{240}$ change takes longer than 20 min. The increasing $\Delta\epsilon_{240}$ values with time at low pH are likely to bias titration fits toward decreased pK_a values and increased molar absorptivities for the high-pK_a titrating tyrosines (vide infra). Thus, it was essential to promptly measure the absorption and Raman spectra immediately after the protein solution was taken to pH values greater than ca. 12.7.

Results

Figure 1 shows the pH dependence of the absorption spectra of solutions containing tyrosine, tryptophan, and phenylalanine

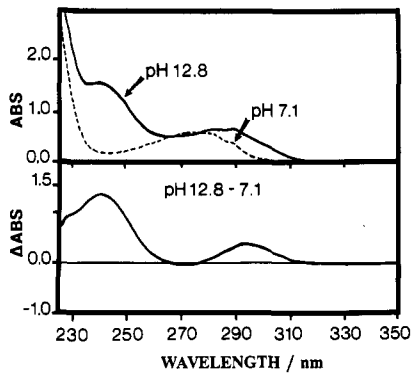

FIGURE 1: Absorption spectra of mixtures of aromatic amino acids at pH 7.1 and 12.8 and their difference spectrum. The amino acid relative concentrations are identical with those present in sperm whale myoglobin solution: 0.6 mM Tyr, 0.4 mM Trp, 1.2 mM Phe, 30.0 mM phosphate buffer, and 250 mM $NaClO_4$. Path length is 1 cm.

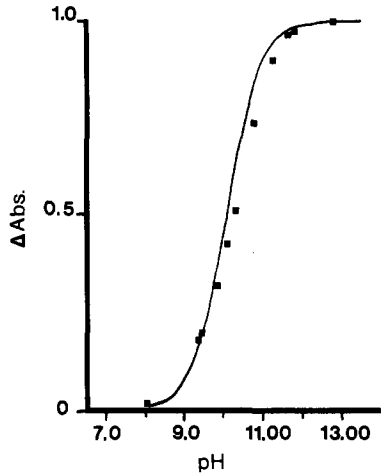

FIGURE 2: UV absorption difference titration behavior of tyrosine at 240 nm in a mixture of the aromatic amino acids. The solution concentrations are given in the Figure 1 caption.

at relative concentrations identical with those in sperm whale myoglobin. The spectral shifts observed (highlighted in the difference spectrum) derive from deprotonation of the tyrosyl residues to form tyrosinate. The tyrosine L_b band shifts from ca. 275 to 295 nm while the L_a band shifts from 225 to 240 nm and increases its molar absorptivity (Demchenko, 1986). Essentially all of the difference spectral features derive from the conversion of tyrosine to tyrosinate. Although both the L_b and L_a absorption spectral shifts could be used to monitor tyrosine titrations, the absorption increase at ca. 240 nm is generally used for protein studies because it is freer from interferences from absorption spectral alterations of other protein constituents such as tryptophan, tyrosine, and phenylalanine (Uyeda & Peisach, 1981; Nagel et al., 1966). Figure 2, which shows the titration behavior of the absorbance at 240 nm, displays a simple behavior associated with the titration of a single species with a pK_a of 10.0.

The 240-nm excited resonance Raman spectrum of this mixture of aromatic amino acids at pH 12.4 and 8.0 is shown in Figure 3. The Raman band at 932 cm^{-1} arises from the symmetric stretch of the perchlorate anion (Dudik et al., 1985b). The UV resonance Raman excitation profile maximum of tyrosinate in water occurs at tyrosinate's 240-nm absorption spectral maximum (Asher et al., 1986). Although the 240-nm excited UVRR spectrum of the aromatic amino acid mixture at pH 12.4 is dominated by the resonantly enhanced tyrosinate bands, some weaker contributions are also evident from tryptophan and phenylalanine. The 240-nm

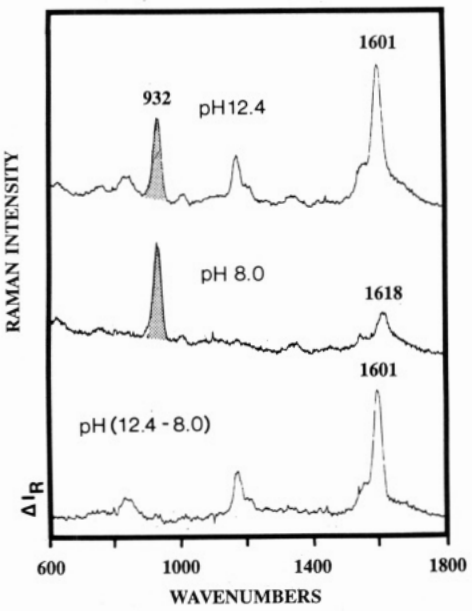

FIGURE 3: UV resonance Raman spectra of the aromatic amino acids excited at 240 nm at pH 8.0 and 12.4 and their difference spectrum. Concentrations as in Figure 1. The internal standard perchlorate band at 932 cm^{-1} is shaded.

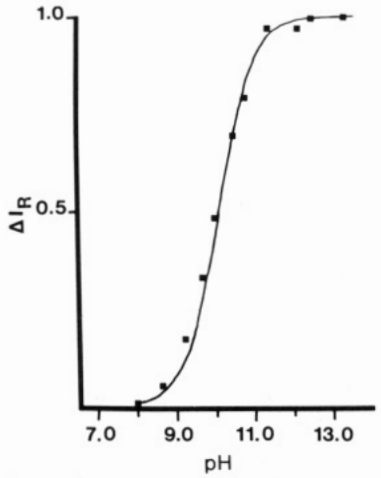

FIGURE 4: 240-nm UV resonance Raman difference titration behavior of tyrosine in a mixture of aromatic amino acids. Conditions as in Figure 2. The relative Raman intensities were obtained by peak height measurements of the tyrosinate 1601 cm^{-1} band and the 932 cm^{-1} internal standard.

Raman spectrum of the same aromatic amino acid mixture at pH 8.0 shows more clearly the off-resonance contributions of tyrosine, tryptophan, and phenylalanine. The pH 12.4–8.0 Raman difference spectrum shows the Raman bands only from the resonantly enhanced tyrosinate species. The spectra were scaled prior to subtraction such that the intensities of the perchlorate internal standard were identical. The peak at 1601 cm^{-1} and the shoulder at 1556 cm^{-1} are assigned to the ν_{8a} and ν_{8b} in-plane stretching mode of tyrosinate. The 1175 cm^{-1} band is an in-plane CH bending mode that resembles the ν_{9a} mode of benzene, and the shoulder at 1208 cm^{-1} is a symmetric ring stretching mode which is commonly observed in para-substituted benzene derivatives. The unresolved doublet at ca. 850 cm^{-1} in tyrosinate derives from the Fermi resonance between the symmetric ring stretching fundamental (ν_1) and the first overtone of the out-of-plane ν_{16a} ring deformation mode (Asher et al., 1986; Hildebrandt et al., 1988). This unresolved doublet has been used in normal Raman protein studies to monitor the tyrosyl environment.

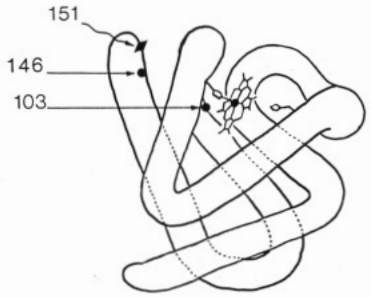

FIGURE 5: Tertiary structure of myoglobin and the location of tyrosine residues 103, 146, and 151. Adapted from Uyeda and Peisach (1981).

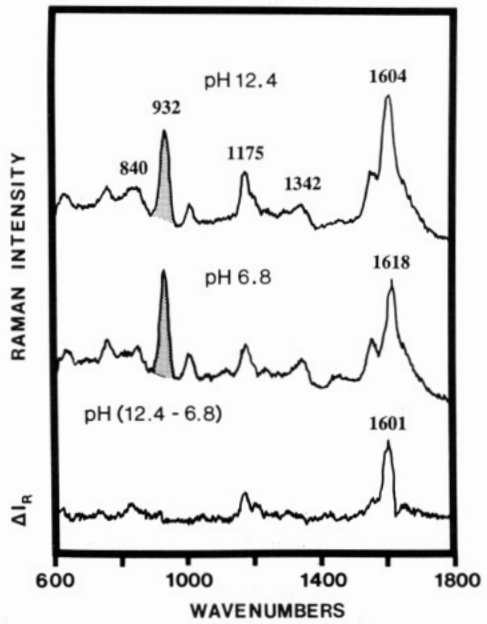

FIGURE 6: UV resonance Raman spectra of sperm whale myoglobin excited at 240 nm at pH 6.8 and 12.4 and the difference spectrum. Concentrations: 0.17 mM in heme, 30 mM phosphate buffer, and 250 mM sodium perchlorate. The internal standard perchlorate band at 932 cm^{-1} is shaded.

The intensity ratio of the ca. 1601 cm^{-1} tyrosinate band relative to the 932 cm^{-1} internal standard band exhibits a simple pH titration behavior (Figure 4). The UV absorption difference and the UV resonance Raman difference spectral pH titrations of the aromatic amino acid mixtures shown in Figures 2 and 4 both exhibit pK_a values of 10.0 ± 0.1, which compares favorably to the literature aqueous tyrosine pK_a value of 10.03 (Demchenko, 1986).

Figure 5 schematically shows the tertiary structure of horse and sperm whale myoglobin and the locations of the tyrosine residues. Horse myoglobin has tyrosyl residues at positions 146 and 103, while sperm whale myoglobin has tyrosyl residues at positions 151, 146, and 103 (Dayhoff, 1976). The *different* environments for the *different* tyrosyl residues in these myoglobins result in a more complex tyrosine titration curve than observed for the aromatic amino acid aqueous solutions. Unique pK_a values occur for each of tyrosine residues.

The 240-nm excited resonance Raman spectra of sperm whale myoglobin (Figure 6) at pH 12.4 and 6.8, as well as their difference spectrum, are similar to those of the aromatic amino acid mixture (Figure 3). However, a comparison between the pH 6.8 sperm whale myoglobin spectrum and the pH 8.0 aromatic amino acid mixture spectrum clearly displays an increased complexity for the protein spectrum. The additional Raman bands in the protein spectrum partially derive from an increased relative enhancement of the tryptophan residues (ca. 760, 1006, and 1550 cm^{-1} bands). Apparently,

Table I: *N*-Acetyl-L-tyrosinamide Absorption and Raman Spectral Parameters

parameter	solvent	
	H_2O	90% ethylene glycol
ϵ (mM^{-1} cm^{-1})	11.6	13.0
λ_{max} (nm)	241.4	244.0
σ^a	0.31	0.39[b]
n^c	1.39	1.52

[a] Raman cross section of 1601 cm^{-1} band [b/(mol·sr)] at 240-nm excitation. [b] Estimated from local field data of Larkin et al. (1990). [c] Extrapolated refractive index from glycerol (Brikhoff et al., 1974).

the tryptophyl protein environments result in increases in their relative UVRR cross sections for 240-nm excitation. The UVRR difference spectrum of the sperm whale myoglobin, in contrast, shows only the resonantly enhanced Raman bands of tyrosinate since the other bands subtract out.

In order to examine the effect of environment on the tyrosinate electronic transition, we compared the absorption spectra of high-pH solutions of *N*-acetyl-L-tyrosinamide (NATYR) between water and ethylene glycol. Table I lists the absorption λ_{max} and the molar absorptivities of NATYR in water and 90% ethylene glycol. The 241.4-nm peak maximum of NATYR in water red-shifts to 244.0 nm in the ethylene glycol solution and shows a 12% increased molar absorptivity. Table I also lists the Raman cross sections at ca. 240-nm excitation of the NATYR species in water and ethylene glycol (Larkin et al., 1990). The Raman cross sections in ethylene glycol increase by ca. 25% compared to that in water. Excitation occurred at the absorption maximum of the NATYR in each solution.

Figures 7 and 8 show UV absorption difference (UVAD) and the UV resonance Raman (UVRR) pH titrations of horse and sperm whale myoglobin. The UVAD pH titration shows the change in the absorbance at the λ_{max} of the tyrosinate band (247 nm) as a function of pH. The UVRR difference titration displays the pH dependence of Raman intensity (ΔI_R) of the 1601 cm^{-1} tyrosinate band relative to the 932 cm^{-1} internal standard. The UVAD pH titration data were modeled by using a nonlinear least-squares fit of an expression which included independent terms for the titration of the different tyrosine residues (two for horse and three for sperm whale myoglobin). The UVAD titration model fits shown in Figures 7 and 8 yield pK_a values for 10.2 and 12.9 for horse myoglobin and pK_a values of 9.9, 11.7, and 13.4 for sperm whale myoglobin.

The sperm whale myoglobin pK_a values are acceptably similar to those previously reported pK_a values of 10.3, 11.8, and 12.9 by Uyeda and Peisach (1981) given the differences in the titration model used (vide infra). On the basis of previous studies (Hermans, 1962; Wilbur & Allerhand, 1976; Uyeda & Peisach, 1981), we assign the tyrosine with a pK_a of 9.9 to residue 151, the pK_a of 11.7 to residue 103, and that with a pK_a of 13.4 to residue 146. Table II lists the pK_a values and the molar absorptivities that our model calculates for the different tyrosyl residues of sperm whale and horse myoglobin. The pK_a value for the sperm whale myoglobin penultimate tyrosine-151 is essentially identical with the pK_a value of 10.0 obtained for aqueous tyrosine. Further, tyrosinate-151 shows

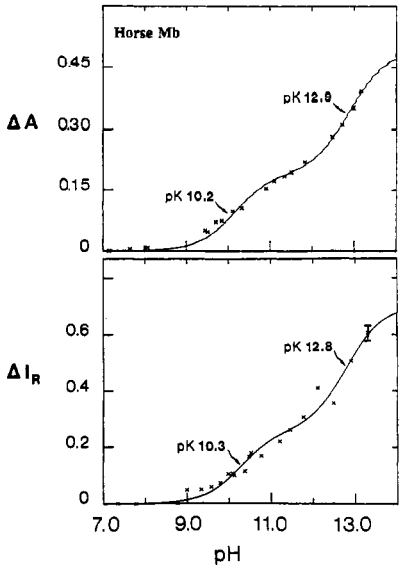

FIGURE 7: Titration of tyrosine residues in horse myoglobin monitored by UV resonance Raman and UV absorption difference spectroscopy. The myoglobin concentration was 0.17 mM in heme for the UVRR study and 0.075 mM for the UVAD study. The concentration of the sodium perchlorate was 250 mM, and the solutions contained 30 mM phosphate and sodium bicarbonate. The solid curves are the nonlinear least-squares fits as discussed in the text.

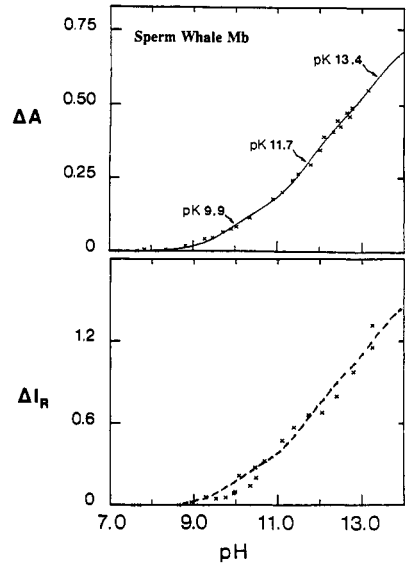

FIGURE 8: Titration behavior of tyrosine residues in sperm whale myoglobin monitored by UV resonance Raman and UVAD spectroscopy. The solid curve for the absorption pH titration is the nonlinear least-squares fit as discussed in the text. The dashed curve in the Raman pH titration is identical with that for the absorption titration. The myoglobin concentration was 0.17 mM for UVRR and 0.0835 mM for the UVAD study and the solutions contained 0.25 M sodium perchlorate, 30 mM sodium phosphate, and 30 mM sodium bicarbonate.

Table II: Titration Parameters for Horse and Sperm Whale Myoglobin

residue	sperm whale pK_a	ϵ^a	σ^e	comments	horse pK_a[b]	ϵ^c	σ^d	comments
151	9.9	8.9	0.18	half-exposed to H_2O, no nearby aromatic residues				
146	13.4	17.2	0.41	in alkane cage, no close aromatics	12.9	20.1	0.28	Phe replaces Tyr-151, probably close to Tyr-146
103	11.7	18.5	0.47	many aromatic residues around tyrosyl, partially exposed to H_2O, but mostly enclosed	10.2	12.7	0.17	probably highly exposed to aqueous environment

[a] mM^{-1} cm^{-1}. [b] From Raman: 146 – pK_a = 12.8; 103 – pK_a = 10.3. [c] $\epsilon_{146}/\epsilon_{103}$ = 1.58. [d] $\sigma_{146}/\sigma_{103}$ = 1.65. [e] From nonlinear least-squares fit using the pK_a values determined from the absorption spectrum.

a low molar absorptivity (8.9 mM^{-1} cm^{-1}) close to that of aqueous tyrosinate (11.6 mM^{-1} cm^{-1}), as is expected due to its high exposure in the protein to the aqueous environment. In contrast, the other tyrosine residues demonstrate higher pK_a values and ca. 2-fold increased molar absorptivities.

Our horse myoglobin pK_a value of ca. 12.9 agrees well with that from Uyeda and Peisach (1981), and we similarly assign this pK_a value to tyrosine residue 146. We assign the lower pK_a value of 10.3 to tyrosine-103. Our measured pK_a of 10.3 which is close to that of free tyrosine differs dramatically from the value obtained by Uyeda and Peisach of 11.4. Both the UVAD and the UVRR titration study of horse Mb yields a pK_a value of 10.3 for this tyrosyl residue. Our results for horse myoglobin differ significantly from that of Uyeda and Peisach (1981) because we use a different model for the pH titration which is more physically reasonable than theirs (vide infra). We obtain results similar to Uyeda and Peisach's when we use their model to fit our titration data.

We were unable to satisfactorily fit the sperm whale myoglobin UVRR titration data with our titration model. The protein structural changes that accompany the pH changes may affect the Raman intensities (Acampora & Hermans, 1967a,b; Ragone et al., 1984, 1987) to such a degree that the simple model is insufficiently robust to numerically converge within the spectral signal-to-noise ratios. However, the dashed curve shown in the Raman titration, which is a scaled version of the absorption spectral titration fit (vide infra), excellently models the Raman data.

Compared to aqueous tyrosinate (*N*-acetyl-L-tyrosinamide), tyrosinates-146 and -103 of horse myoglobin have larger molar absorptivities [compare Tables I and II and Asher et al. (1986)] and show a ca. 7 (5) nm red shift of their λ_{max} values [compare Tables I and III and Asher et al. (1986)]. The 240-nm excited Raman cross section of the 1601 cm^{-1} tyrosinate band is decreased in horse myoglobin by 26% (10%) and 55% (45%) for tyrosinate-146 and tyrosinate-103 compared to aqueous tyrosinate (*N*-acetyl-L-tyrosinamide) solution. This Raman cross section decrease derives almost entirely from the protein-induced L_a absorption spectral red shift away from the excitation wavelength. Aqueous tyrosinate shows an excitation profile maximum at 240 nm with a cross section of 0.38 b/(sr·mol). A 7-nm red shift of the absorption and a similar 7-nm red shift of the excitation profile would result in a 240-nm excitation Raman cross section for the 1601 cm^{-1} band of 2.3 b/(sr·mol), a 39% decrease (Asher et al., 1986). Tyrosinate-146 of horse myoglobin has a 58% larger molar absorptivity and a 65% larger Raman cross section than does tyrosinate-103. It appears that an increased tyrosine pK_a value is accompanied by an increased molar absorptivity and Raman cross section. Tyrosyl residues 146, which have the highest pK_a values of 13.4 in sperm whale and 12.8 in horse myoglobin, have the largest molar absorptivities. In contrast, tyrosine-103 of horse myoglobin shows a pK_a only slightly elevated over that of aqueous tyrosine and a molar absorptivity only slightly increased over that of aqueous tyrosinate. The environment of tyrosine-103 must differ for sperm whale myoglobin compared to horse myoglobin since in sperm whale myoglobin this residue shows a pK_a of 11.7 and a molar absorptivity of 18.5 mM^{-1} cm^{-1} and in horse myoglobin shows a pK_a of 10.2 and a molar absorptivity of 12.7 mM^{-1} cm^{-1}. The penultimate tyrosine-151 of sperm whale myoglobin has the lowest pK_a (9.9), the lowest molar absorptivity, and the lowest Raman cross section.

Figure 9 shows the horse myoglobin pH absorption difference spectra in pH ranges where only tyrosine-103 titrates;

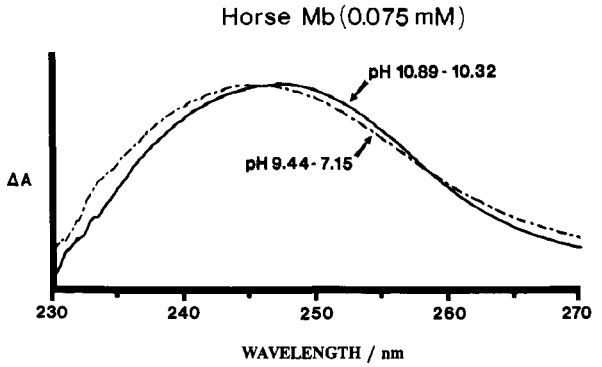

FIGURE 9: pH 10.89–10.32 and pH 9.44–7.15 UV absorption difference spectra of horse myoglobin. Conditions identical with those in Figure 8.

Table III: Apparent Molar Absorptivity and Increased Tyrosinate Concentration as a Function of the pH Range Titrated for Horse Myoglobin[a]

pH range	λ_{max} (nm)	ϵ^b	ΔC_{103} (mM)	ΔC_{146} (mM)
7.15–9.44	245	12	0.0158	0.000
10.32–10.89	247.5	9.7	0.019	0.001
10.89–11.33	247	17	0.008	0.001
11.08–11.49	247.5	14	0.005	0.002

[a] Myoglobin concentration is 0.075 mM. [b] mM^{-1} cm^{-1}.

because tyrosine-103 has a pK_a of 10.2, it selectively titrates in the region between pH values of 9.0 and 11.0. Tyrosine-146 with a pK_a of 12.9 only begins to titrate at pH values above 11.0. Changes in the λ_{max} and the ϵ_{max} values are observed for the tyrosinate-103 residue between the pH 9.4 and pH 10.5 ranges. The molar absorptivities for the titrating tyrosines in the different pH regions were calculated from the absorption difference spectra and the calculated concentrations of tyrosinates formed in the two pH ranges (see Table III). The tyrosinate concentrations were calculated from the pK_a values determined in this study.

The fact that the absorption maximum red shifts by ca. 2.5 nm and the molar absorptivity decreases by 21% between the pH ranges of ca. 9.4 and pH 10.5 clearly indicates a complex titration behavior for the protein; solution pH increases cause both heme ligation changes due to binding of hydroxide and protein structural changes which influence the tyrosinate electronic transitions due to an evolution of the tyrosinate environment (Acampora & Hermans, 1967a,b). The pH dependence of the tyrosinate absorption of sperm whale myoglobin is much more complex than that of the horse myoglobin. At the lowest pH measured at ca. 9.8, λ_{max} occurs at 252 nm, but shifts to 248 nm at pH 10.0, to 246 nm at pH 11.2, and to ca. 250 nm at pH 11.7, but to ca. 245 nm at pH 12.0. This pH-induced evolution of the tyrosinate environment is likely to be responsible for our inability to fit the Raman cross-section titration data for sperm whale myoglobin using a simple model; the Raman cross sections are likely to be more sensitive to changes in the tyrosinate environment (vide infra). The pH evolution of the protein structure at these pH values must derive from titrations of residues in addition to the tyrosines (Shire et al., 1975; Friend & Gurd, 1979) and to partial unfolding of the protein at the highest pH values (Hirsch & Peisach, 1986).

Discussion

Tyrosine pK_a Values. The spectral changes observed during the protein titration can potentially yield detailed information on alterations in the tyrosine and tyrosinate environments

(Demchenko, 1986). In order to characterize the tyrosine environment through the spectral data, we must first quantitatively relate the Raman and absorption spectral parameters to specific interactions such as hydrogen bonding, for example, and to less specific interactions such as hydrophilicity and hydrophobicity and the effective dielectric constant of the environment (Asher, 1988). The quantitative relationships between the absorption and Raman cross sections and the tyrosinate environments are relatively complex.

The dependence of the absorption λ_{max} values on protein environment has been extensively characterized in numerous previous studies (Yanari & Bovey, 1960; Grinspan et al., 1966; Bailey et al., 1968), as have the dependences of the tyrosine Raman frequencies and bandshapes upon hydrogen bonding (Takeuchi et al., 1989; Siamwiza et al., 1975; Harada, 1986; Liu et al., 1989; Hildebrandt et al., 1988). However, far less attention has been paid to the dependence of the molar absorptivities and Raman cross sections upon environment. A strong environmental dependence of the absorption and Raman cross sections is clearly evident from our titration data.

We can theoretically partition the environmental dependence of the absorption and Raman cross sections into different phenomenological sources. Experimentally, this can be accomplished by comparing the Raman cross sections, the Raman excitation profile bandshapes, and their λ_{max} values to the absorption cross sections, the absorption bandshapes, and the absorption λ_{max} values.

To relate the measured absorption spectral data to single tyrosine environments, we must deconvolute measured absorption spectra into the absorption bands of the individual tyrosyl residues. Since there are multiple tyrosine residues in the protein and since some absorption spectral changes are derived from protein structural alterations which are not directly coupled to tyrosine titrations, we can write the following relationship for $A(\lambda)$, the tyrosine absorbance at wavelength λ:

$$A(\lambda) = l\sum_i \epsilon_i(\lambda)C_i \quad (1)$$

where l, ϵ_i, and C_i are the sample path length, the molar absorptivity of tyrosyl residue i at wavelength λ, and the concentration of residue i, respectively.

A similar expression can be written for the Raman intensity at Raman frequency $\hat{\nu}$ for excitation at ν_0:

$$I(\hat{\nu},\nu_0) = K(\nu,\hat{\nu}_0)I_0\sum_i \sigma_i(\nu,\hat{\nu}_0)C_i \quad (2)$$

where $K(\hat{\nu},\nu_0)$ is an instrumental factor associated with the scattered light collection solid angle and the illuminated sample volume. It contains the instrument transfer function as well as any sample self-absorption bias. I_0 is the incident laser photon flux, and $\sigma_i(\hat{\nu},\nu_0)$ is the Raman cross section of species i.

A change in the solution conditions such as a change in the pH results in absorption and Raman intensity changes given by

$$\Delta A(\nu) = l\left\{\sum_i\left[C_i\frac{\partial\epsilon_i(\nu)}{\partial pH} + \epsilon_i(\nu)\frac{\partial C_i}{\partial pH}\right]\right\}\Delta\text{pH} + \ldots \quad (3)$$

and

$$\Delta I(\hat{\nu},\nu_0) = I_0\frac{\partial K(\hat{\nu},\nu_0)}{\partial pH}[\sum_i \sigma_i(\hat{\nu},\nu_0)C_i] + K(\nu,\nu_0)\sum\left[\frac{\partial\sigma_i(\hat{\nu},\nu_0)}{\partial pH}C_i + \sigma_i(\hat{\nu},\nu_0)\frac{\partial C_i}{\partial pH}\right]\Delta\text{pH} + \ldots \quad (4)$$

The terms explicitly displayed in eq 3 and 4 give the linear pH dependence of the absorption and Raman spectra. Any nonlinear dependence would involve higher order terms.

The linear absorption spectral changes are associated with changes in the concentrations of residues (e.g., titration of tyrosine to tyrosinate) as well as with alterations in the molar absorptivity of the tyrosinates and alterations in the molar absorptivities of nontitrating residues due to local environmental changes which accompany pH-induced protein conformational changes (Ragone et al., 1984, 1987).

The linear Raman intensity changes include three terms. Similar to absorption, we have terms which express the Raman cross-section changes and the residue concentration changes. The additional first term involves optical changes in the sample which lead to changes in the illuminated sample volume and the transmittance of light out of the sample. These changes derive from changes in self-absorption (Ludwig & Asher, 1988b) due to pH-induced absorption spectral changes. This term is negligibly small for the study reported here. The term which displays the cross-section dependence upon pH is limited to changes only in the tyrosyl residues.

For the absorption spectral changes in myoglobin monitored at ca. 247 nm, we are mainly sensitive to changes in the concentration of tyrosinate, which is the only species with a distinct absorption band in this spectral region (Demchenko, 1986; Uyeda & Peisach, 1981). Thus, we can fit our experimental titration data with a simplified version of eq 3, subject to the constraint that the only species of interest which give rise to absorption spectral *changes* at ca. 247 nm are tyrosinate residues:

$$\Delta A = l\sum_j\left[\epsilon_j\Delta C_j + C_j\frac{\partial\epsilon_j}{\partial pH}\right] \quad (5)$$

where the summation occurs only over the different tyrosinate residues of the protein. We ignore the contribution of tyrosines since they have negligible absorption around 247 nm. The concentration of each tyrosine is subject to the constraint

$$C_{Tyr^-} = C_T - C_{Tyr} \quad (6)$$

where C_T, C_{Tyr^-}, and C_{Tyr} are the total tyrosyl concentration, the concentration in the tyrosinate form, and the concentration in the tyrosine form, respectively. The Henderson–Hasselbach relationship details the relative tyrosinate concentration at any pH, given a well-defined pK_a value:

$$C_{Tyr^-} = \frac{C_T}{1 + 10^{pK_a - pH}} \quad (7)$$

We can experimentally determine the tyrosyl pK_a values by a nonlinear least-squares fit of eq 5 where we neglect the smaller second term and where we utilize eq 7 for each of the tyrosyl residues and allow ϵ_i to differ between residues. For the horse and sperm whale myoglobin, we assume two and three independently titrating tyrosines, respectively. From Figure 9 and Table III, we recognize that this is not strictly correct since the molar absorptivity of each tyrosinate residue is changing with pH.

Our titration model differs fundamentally from that of Uyeda and Peisach (1981) since they include an additional titrating term to account for any 240-nm absorption spectral changes due to alterations in the heme adsorption due to ligation of hydroxide at higher pHs. Surprisingly, they find a spectral change with an apparent pK_a of ca. 9.0 which has $\Delta\epsilon$ values ca. 50% of that for a titrating tyrosinate. This result is likely to be artifactual since the heme absorption is relatively small and featureless at 240 nm (DeVito & Asher, 1989). Ligation changes should result in insignificant heme absorption

spectral changes. In our titrations, we have utilized numerically calculated difference spectra in which $\Delta\epsilon_{240}$ is measured above a horizontal base line which effectively removes any broad absorption spectral shifts due to heme absorption changes due to hydroxide ligation (see Figure 9).

The additional phenomenological term used by Uyeda and Peisach would indeed result in an improved fit to the ca. pH 9 absorption *and* Raman titration data. Figure 7 shows significant deviation for horse Mb between the measured and calculated titration data around ca. pH 9.0. In fact, if we add an additional term, we calculate an identical pK_a of 9.2 as that of Uyeda and Peisach. The fact that the absorption difference and Raman data are *only* sensitive to tyrosinate formation indicates the existence of a complex titration behavior for tyrosine around ca. pH 9.0. We suggest that the tyrosine-103 pK_a is being altered as hydroxide binds and replaces the neutral H_2O ligand present at lower pH. This supposition is completely supported by Uyeda and Peisach's titration results for the cyanide derivative of horse Mb. No evidence for a pK_a 9.0 titrating spectral change is present for this ligand which remains bound at all pH values. In contrast, the Tyr-103 pK_a of the fluoride derivative shifts ca. 0.4 pH unit above that for the aquo complex. In addition, since hydroxide competes with fluoride at high pH values, an additional titrating absorption feature is found at a pK_a of 9.5. In summary, our data only report on titration of tyrosines. Binding of hydroxide apparently increases the Tyr-103 pK_a. Thus, we determine a pK_a value for Tyr-103 which represents an averaged value associated with a tyrosine titration which is complicated by heme ligation changes and pH-induced protein structural alterations.

As illustrated in Figures 7 and 8, we obtain adequate fits to the absorption titration curves and obtain pK_a values of 10.2 and 12.9 for horse myoglobin and 9.9, 11.7, and 13.4 for sperm whale myoglobin. For the horse myoglobin, the model calculates a molar absorptivity value for each tyrosinate which is an average of the value that each tyrosinate residue displays over its pH titration range. It should be noted that the absorption spectral data used to construct the titration curves of Figures 7 and 8 derive only from the tyrosinate residues; in contrast, absorption spectral changes at ca. 220 nm would monitor the tyrosines. As discussed above, eq 5 and 7 used to model our titration data differ fundamentally from that used by Uyeda and Peisach (1981). Our model utilizes fewer parameters, but explicitly demands that all the absorption and Raman spectral changes at ca. 240 nm result from the appearance of tyrosinate.

Our results show that the distinct tyrosinate environments giving rise to different pK_a values for different tyrosinate residues also have associated with them different tyrosinate molar absorptivities (see Results); tyrosyl residues with higher pK_a values show larger molar absorptivities. As indicated in Table I, tyrosinates in more hydrophobic environments display larger molar absorptivities than those in aqueous environments. Because hydrophobic environments correlate with red shifts of the λ_{max} values (Bailey et al., 1968), we can tentatively conclude that the higher pK_a tyrosines occur in more hydrophobic environments.

The origin of the absorption spectral environmental dependences for the aromatic amino acids has been the subject of numerous studies (Ragone et al., 1987, 1984; Balestrieri et al., 1978; Williams, 1966; Acampora & Hermans, 1967a,b; Yanari & Bovey, 1960; Bailey et al., 1968). The studies which have concentrated on phenylalanine, tyrosine, and tryptophan have suggested that the spectral shifts are related to changes in dispersive interactions, electrostatic interactions due to nearest-neighbor dipolar or charged residues, hydrogen bonding, and relative shifts in the electron density of the ground and excited states due to changes in hydrogen bonding (Demchenko, 1986). These studies have not reached clear quantitative correlations, and none of these studies examined tyrosinate, the subject of the study here. We conclude from this body of work that there is a dependence of the λ_{max} and molar absorptivity on the solvent polarizability (measured by the refractive index) and a dependence associated with hydrogen-bonding interactions and the proximity of charged groups. We will attempt to quantitatively begin a partitioning of these effects in this study.

To complicate any analysis of the pH dependence of the tyrosinate absorption, we must incorporate the results in Figure 9 which shows a blue shift for tyrosine-103 and a decrease in the molar absorptivity as the pH increases. Both of these alterations are indicative of protein conformational changes that lead to more hydrophilic tyrosine-103 environments as the pH varies from 9.44 to ca. 10.6. This indicates that as the pH increases and the heme and other protein residues titrate, the horse myoglobin responds by permitting the tyrosinate-103 environment to become more exposed to the aqueous environment. The titration behavior of the tyrosyl residues is quite complex as evident from the changes in the molar absorptivity for the titrating tyrosinate residues in different pH ranges. Table III lists the concentrations of tyrosinates formed for different pH ranges as well as their molar absorptivities and their λ_{max} values calculated from the horse myoglobin absorption spectral changes. Obviously, those tyrosinate-103 residues titrating in the pH 10.32–10.89 range are in a more aqueous environment compared to those titrating in the lower pH range as evident from their decreased molar absorptivity. However, it should be noted that this molar absorptivity value is a function both of the molar absorptivity of the newly titrated tyrosine-103 residues and also of any molar absorptivity changes for tyrosinates previously formed. As the pH increases, the molar absorptivity of previously titrated residues could decrease if their environment becomes more hydrophilic. At the higher pH values, the molar absorptivity increases because of the increasing contribution of the titration of tyrosine residue 146 which is in a more hydrophobic environment. The higher molar absorptivity displayed in the pH 10.89–11.33 range presumably signals a protein conformational change which places the tyrosinates in a more hydrophobic environment.

We can successfully model the Raman pH titration behavior of the horse myoglobin tyrosines by utilizing only the third term of eq 4 and neglecting the smaller first two terms. Thus, for horse myoglobin, the changes in the Raman cross section of each tyrosinate upon pH alterations are averaged out over the titration. This permits the model to accurately fit the titration data and to extract reasonably accurate pK_a values. We find that the Raman cross sections of the two tyrosinates differ by ca. 70%.

For horse myoglobin, we derive essentially the same pK_a values from Raman data as from the absorption data. Satisfyingly, the Raman cross sections of the tyrosines differ in the same direction as their molar absorptivities. The higher pK_a residue has a 1.65-fold higher Raman cross section and an associated 1.58-fold higher molar absorptivity.

Even though we are successful in modeling both the absorption and Raman pH titration behavior of horse myoglobin, we are unable to successfully model the sperm whale myoglobin Raman titration data using a similar approach. Our nonlinear model fit is not sufficiently robust and does not

uniquely converge. This presumably results from the dependence of the Raman cross sections upon the pH-induced changes in the tyrosinate absorption. The sperm whale myoglobin tyrosinate absorption shows a very complex pH dependence. It is satisfying, however, that a titration plot using the absorption titration pK_a values and using Raman cross-section values proportional to the molar absorptivity values gives a calculated Raman titration curve that fits the data well. Surprisingly, the tyrosinate Raman cross-section ratios for both the horse and sperm whale myoglobin are almost in proportion to their respective molar absorptivities.

Tyrosinate Molar Absorptivities and Raman Cross Sections. The absorption molar absorptivities and the absorption bandshape, as well as the Raman cross sections and the Raman excitation profiles, depend upon the excitation frequency, the vibronic transition moments, the local dielectric constant, and the homogeneous and inhomogeneous line widths (Asher, 1988; Myers & Mathies, 1987). The dependences upon these parameters differ, in general, between these two spectroscopies. However, almost identical dependences upon these parameters can occur for the Raman excitation profiles and the absorption spectrum upon spectral shifts and upon changes in the inhomogeneous line width under conditions where inhomogeneous broadening dominates (a common occurrence). For example, an increase in the number of tyrosine environments will result in an increase in the inhomogeneous line width which increases the bandwidths of both the absorption spectrum and the resonance Raman excitation profile; the maximum molar absorptivity and Raman cross section will proportionately decrease. On the other hand, if inhomogeneous broadening does not dominate, then the Raman cross-section excitation profile alterations will not be in proportion to the molar absorptivity changes.

The quantitative dependence of the absorption spectra and the Raman cross sections upon the inhomogeneous line width is derived from the convolution of the population distribution function, $G(\nu_i)$, with the intrinsic molar absorptivity and the Raman cross section:

$$\epsilon(\nu) = \int \epsilon_0(\nu - \nu_i)G(\nu_i)\, d\nu_i \tag{8}$$

$$\sigma(\hat{\nu},\nu_0) = \int \sigma_0(\hat{\nu},\nu_0 - \nu_i)G(\nu_i)\, d\nu_i \tag{9}$$

where we have assumed the simplest case, where changes in the inhomogeneous distribution lead only to alterations in the transition frequencies and do not affect spectroscopic properties such as homogeneous line widths and oscillator strengths.

The absorption cross section σ_A (cm^2/molecule) is related to the molar absorptivity (M^{-1} cm^{-1}) as

$$\sigma_A = 2303\epsilon/N_A \tag{10}$$

where N_A is Avogadros number. The absorption cross section (Myers & Mathies, 1987) to lowest order is given as a function of frequency, ν_0, as

$$\sigma_A(\nu_0) = K\Xi_A\nu_0\Gamma\sum_v \frac{|\langle e|\mu|g\rangle\langle v|i\rangle|^2}{(\nu_{ev} - \nu_0)^2 + \Gamma^2} \tag{11}$$

where K is a numerical prefactor. Ξ_A is a parameter which is determined by the local electromagnetic field strength incident on the absorbing species. As discussed later, the value of Ξ_A depends upon the local environmental refractive index as well as the polarizability of the absorbing species. ν_0 is the excitation frequency, Γ is the homogeneous line width, $\langle e|\mu|g\rangle$ is the electronic transition moment between the ground state, g, and the electronic excited state, e, and $\langle v|i\rangle$ is the Franck–Condon factor between the initial vibrational level i of the ground state and the vibrational level v of the excited state.

The resonance Raman cross section (Asher, 1988; Myers & Mathies, 1987) shows a higher order dependence on these spectroscopic parameters:

$$\sigma(\hat{\nu},\nu_0) = K_2\Xi_R(\nu_0 - \hat{\nu})\nu_0^3\sum_{ev}\left|\frac{\langle f|\mu|e\rangle\langle e|\mu|g\rangle\langle f|v\rangle\langle v|i\rangle}{\nu_{ev} - \nu_0 - i\Gamma_{ev}}\right|^2 \tag{12}$$

where K_2 is a numerical prefactor and Ξ_R is the parameter which scales the Raman cross section for the effective local electromagnetic field strength of the excitation beam.

Both the absorption and Raman spectra depend upon the transition moment to the resonant excited state. Whereas the absorption shows a squared dependence on the electronic transition moment, the Raman cross section depends on the fourth power of the transition moment (Myers & Mathies, 1987). Furthermore, the Raman cross section shows a higher order dependence both on the homogeneous line width and on the vibrational Franck–Condon factors.

If the absorption line width is dominated by inhomogeneous broadening, then it is almost certain that the Raman excitation profile will also be dominated by this inhomogeneous broadening. In this case, the absorption and Raman excitation profile line shapes will be essentially identical, and any change in the molar absorptivity will be accompanied by a proportional change in the Raman cross section. Absorption spectral shifts will be accompanied by identical Raman excitation profile shifts. Indeed, our previous excitation profile measurements of tyrosinate in solution show similar absorption and excitation profile band shapes with only slightly more vibronic structure visible in the excitation profile (Asher et al., 1986; Ludwig & Asher, 1988a). This suggests that for aqueous solutions inhomogeneous broadening is important, if not dominating, in determining the tyrosinate absorption and excitation profile bandshapes. In contrast, the Raman excitation profile of tyrosine differs from its absorption bandshape and is red shifted (Asher et al., 1986; Ludwig & Asher, 1988a). This suggests a smaller relative contribution of inhomogeneous broadening.

In homogeneous broadening is expected to be much more important for tyrosinate than tyrosine in aqueous solutions due to the larger energies associated with electrostatic and hydrogen-bonding interactions for the more highly charged phenoxy oxygen. The smaller hydrogen-bonding interactions of tyrosine would be expected to result in less inhomogeneous broadening and a narrower excitation profile, as is in fact observed (Ludwig & Asher, 1988a).

If inhomogeneous broadening does not dominate, then a more complex relationship will exist between the Raman excitation profile and absorption spectrum. If homogeneous broadening dominates, the excitation profile maximum will scale as the transition moment to the fourth power, and thus as the square of the molar absorptivity. In fact, this scaling is exactly the behavior observed for the tyrosine cross sections in the comparison between monomeric tyrosine and tyrosine in a Tyr-Trp dimer where a hypochromic effect occurs for the Tyr absorption due to excitonic interactions with the Trp (Harmon et al., 1990; Tinoco, 1960; Rhodes, 1961; Bullough, 1965). In contrast, our result that the Raman cross sections in the myoglobin scale in proportion to the molar absorptivity suggests that inhomogeneous broadening dominates.

In general, the Raman and absorption cross sections are described in terms of the isolated resonances; the effective dielectric constant of the surrounding medium is not considered except to the extent that it specifies the transition frequencies by determining the exact energy differences between the ground- and excited-state energies (Bayliss & McRae, 1954;

McRae, 1957). However, it has been well-known for years that the effective dielectric constant of the medium determines the effective field strength of the incident electromagnetic radiation that induces either absorption or Raman scattering (Böttcher, 1973). The local dielectric environment is also responsive to the polarization of the molecule induced by the incident electromagnetic field. This causes an effective rescaling of the local electric field strength whose magnitude depends upon the local dielectric constant (Onsager, 1936; Kirkwood, 1939; Böttcher, 1973).

The simplest model proposed which quantitatively relates the dependence of the absorption and Raman cross sections upon the dielectric environment relates the ratio of the cross sections to the refractive index of the pure analyte and the refractive indices of the local environments (Nestor, 1972; Larkin et al., 1991; Polo & Wilson, 1955; Eckhardt & Wagner, 1966; Mirone, 1966; Nestor & Lippincott, 1973; Abe et al., 1977):

$$\frac{\sigma_A^1(\nu)}{\sigma_A^2(\nu)} = \frac{\Xi_A^1}{\Xi_A^2} = \left(\frac{n_1}{n_2}\right)^3\left(\frac{n^2 + 2n_2^2}{n^2 + 2n_1^2}\right)^2 \quad (13)$$

$$\frac{\sigma_1(\tilde{\nu},\nu_0)}{\sigma_2(\tilde{\nu},\nu_0)} = \frac{\Xi_R^1}{\Xi_R^2} \cong \left(\frac{n_1^2 + 2}{n_2^2 + 2}\right)^4 \quad (14)$$

where n_1 and n_2 are the refractive indices of the two local environments, while n is the refractive index of the pure aromatic amino acid. All of these refractive indices are measured at the excitation frequency, ν_0.

The range of refractive index values for amino acid environments in proteins can be quite large. Previous studies have concluded that the average refractive index for a protein for light in the visible spectral region is around 1.6 (Gilson & Honig, 1986). For UV light, the refractive index should be substantially larger, but there are no studies we are aware of which have quantitated UV protein refractive indices. An aqueous environment would show a ca. UV 240-nm refractive index close to water which is 1.39 (Robinson et al., 1969), while an environment rich in aromatic amino acids and polarizable groups can show refractive indices greater than 1.8 (McRae, 1957; MacRae et al., 1974; Sowers et al., 1972). Extraordinarily large or small refractive indices can occur if the excitation wavelength is within the absorption bands of aromatic amino acids surrounding the tyrosinates. Assuming a refractive index of 1.8, for example, for pure tyrosinate, we calculate an absorption cross-section ratio equal to 1.16 for tyrosinate between an aromatic amino acid rich environment, with an n_1 of 1.8 relative to an aqueous environment with an n of 1.39. However, this same environmental difference yields a Raman cross-section ratio which gives a dramatic 3.15-fold increase in the Raman cross section for a tyrosinate residue in an environment rich in tyrosines and tryptophans compared to an aqueous environment. An increase in the environmental refractive index to 2.0 leads to a similar molar absorptivity increase of 19% relative to an aqueous environment with n = 1.39. However, the Raman cross section continues to increase and is 5.42-fold larger than for an aqueous environment. Obviously, the enhancement of the local electromagnetic field by the dielectric environment results in a much larger effect on the Raman cross sections than on the absorption cross sections. While these effects are expected to be larger, it is important to note that we have recently measured the dispersion of the Raman cross section of benzene, acetonitrile, and hexane in the condensed phase and the gas phase and found no "local field effect" (Harmon & Asher, 1990). In contrast, we find a 25% increase in the Raman cross section of NATYR in a 90% ethylene glycol solution compared to pure water (Larkin et al., 1990).

Myoglobin Tyrosinate Environments. Studies of the tyrosine residue environments using the molecular modeling program TOM and the Cambridge data bank coordinates for aquomet sperm whale myoglobin clearly show that tyrosine-146 is localized in a mainly hydrophobic pocket with little exposure to the aqueous environment. This environment has no nearby aromatic residues; the closest is tyrosine-151 located further than 6 Å away. Thus, we expect a hydrophobic environment with a refractive index of ca. 1.7, which will yield a local field enhancement of 13% for the molar absorptivity and a predicted 2.39-fold enhancement in the Raman cross section compared to that of a tyrosinate completely exposed to aqueous solution.

Both the pK_a values and the molar absorptivities of tyrosinate-146 differ between horse and sperm whale myoglobin (Table II). However, for both proteins, the molar absorptivity is significantly greater than that of aqueous tyrosinate; for horse myoglobin, it is increased by 1.73-fold, while for sperm whale the increase is 1.48-fold. This is much greater than that accounted for by the local field enhancement, and, thus, the increase must derive from other interactions such as hydrogen-bonding or ionic electrostatic interactions which have previously been implicated as being associated with molar absorptivity increases in tyrosine (Bailey et al., 1968; Grinspan et al., 1966). It is not possible at present to specify these ionic or hydrogen-bonding interactions from the neutral protein structure because they are not likely to exist for the neutral tyrosine residue.

The similar Raman cross section of tyrosinate-146 of horse compared to aqueous tyrosinate is surprising in view of our expectation of an almost 2-fold enhancement from the local field increase. The wavelength shift of the tyrosinate absorption band to longer wavelength, away from the excitation, is expected from eq 12 to result in a Raman cross-section decrease. Our previous study of the excitation profile of tyrosinate indicates that a 34% decrease should occur for the 7-nm red shift from that of aqueous tyrosinate monomer. The fact that we see a small net decrease in the cross section, in spite of the molar absorptivity increase and the expected greater than 2-fold local field enhancement, is puzzling and together with the lack of local field effect noted by Harmon and Asher (1990) will be the source for future investigations.

Tyrosine-103 is located in a region which, while partially exposed to the aqueous environment, has numerous close electron-rich residues including phenylalanine-106 and glutamic acid-38. The effective refractive index, which should be at least 1.8, should show a local field enhancement of the molar absorptivity of ca. 16% and a ca. 3-fold Raman cross-section increase. For sperm whale myoglobin, we see a 200% molar absorptivity increase for tyrosinate-103 compared to aqueous tyrosinate. A similar increase is observed compared to penultimate tyrosine-151 which is primarily in an aqueous environment.

A distinctly different result occurs for horse myoglobin tyrosinate-103. Its molar absorptivity is closer to that of aqueous tyrosinate as is its pK_a value. Tyrosinate-103 of horse myoglobin is probably highly exposed to the aqueous solution. We find that the Raman cross section is decreased to 55% of that of aqueous tyrosinate and is slightly more than half of that of tyrosinate-146 of horse myoglobin. Unfortunately, because we could not fit the Raman titration curve of sperm whale myoglobin, we do not accurately know the Raman cross sections of the sperm whale tyrosinates. However, we can

adequately fit the Raman titration using the pK_a values from the absorption titration study and by using relative values of the Raman cross sections which are identical with the relative values found for the molar absorptivities. This is consistent with our observation that for horse myoglobins we have similar ratios of Raman cross sections and molar absorptivities. Thus, sperm whale myoglobin tyrosinates-103 and -146 have similar cross sections both of which should be about 2-fold greater than that of tyrosinate-151.

Although we cannot quantitatively account for the differences in the molar absorptivities and the Raman cross sections between the myoglobin tyrosinates and tyrosinate in aqueous solution, our local field model accounts well for the *relative* cross sections of the protein tyrosinates; the tyrosines in the highest refractive index environment have the highest molar absorptivities and the highest Raman cross section. Indeed, the ratio of Raman cross sections of 1.65 between horse myoglobin tyrosinate-146 and tyrosinate-103 would be identical with the ratio of cross sections between tyrosinate in an $n = 1.57$ environment relative to an $n = 1.39$ aqueous environment. The observed ratio of tyrosinate molar absorptivities is much larger than predicted by eq 13 for a similar refractive index differences.

The results above suggest three possibilities all of which are probably operative: (1) The molar absorptivity depends also upon specific interactions such as ionic interactions and hydrogen-bonding and exciton interactions which change the oscillatory strength of the transition. (2) As previously experimentally noted, the local field expressions often fail to account for the larger changes in absorptivity observed. Thus, the model may be underestimating the electromagnetic field enhancements. (3) We may systematically incorrectly estimate the effective refractive index of the protein environment in the UV. The model which gives the local field enhancement assumes a continuum dielectric. Serious departures from this model may occur if the environment is heterogeneous with aromatic groups close to the tyrosyl residue such as for tyrosinate-103. The appropriate value for the refractive index could be significantly different than that naively expected. This study is the first attempt to estimate local environmental UV refractive indices for proteins. Future studies will attempt to actually measure the refractive indices.

Conclusions

The Raman cross sections show a dependence upon environment similar to that of the absorption cross sections. The observed environmental dependence of the absorption cross sections is larger than that expected from the local field enhancement. In contrast, the dependence of the Raman cross sections is less than that expected. Presumably, specific interactions such as excitonic and ionic electrostatic interactions, as well as hydrogen bonding, are important.

Future studies will examine the tyrosinate excitation profiles as a function of pH. A combination of absorption spectral data, the Raman excitation profiles, and a careful study of the Raman vibrational spectra should allow a deconvolution of the specific phenomena which give rise to the environmental spectral dependence. It should be possible to obtain information both on the average environment as well as on specific interactions such as hydrogen bonding. Other interactions such as excitonic interactions that give rise to hypochromic interactions can also be examined.

Acknowledgments

We thank Serge Alex for preliminary studies relevant to this work and Panos Photinos for his many helpful suggestions with the computer programming.

Registry No. Na-Tyr, 1948-71-6; Tyr, 60-18-4.

References

Abe, N., Wakayama, M., & Ito, M. (1977) *J. Raman Spectrosc. 6*, 38.

Acampora, G., & Hermans, J., Jr. (1967a) *J. Am. Chem. Soc. 89*, 1543–1547.

Acampora, G., & Hermans, J., Jr. (1967b) *J. Am. Chem. Soc. 89*, 1547–1552.

Antonini, E., & Brunori, M. (1971) *Hemoglobin and Myoglobin in Their Reactions with Ligands*, North-Holland Publishing Co., Amsterdam.

Asher, S. A. (1988) *Annu. Rev. Phys. Chem. 39*, 537–588.

Asher, S. A., Johnson, C. R., & Murtaugh, J. (1983) *Rev. Sci. Instrum. 54*, 1657–1662.

Asher, S. A., Ludwig, M., & Johnson, C. R. (1986) *J. Am. Chem. Soc. 108*, 3186–3197.

Bailey, J. E., Beaven, G. H., Chignell, D. A., & Gratzer, W. B. (1968) *Eur. J. Biochem. 1*, 5–14.

Balestrieri, C., Colonna, G., Giovani, A., Irace, G., & Servillo, L. (1978) *Eur. J. Biochem. 90*, 433–440.

Bayliss, N. S., & McRae, E. G. (1954) *J. Phys. Chem. 58*, 1002.

Birkhoff, R. D., Hamm, R. N., Williams, M. W., Arakawa, E. T., & Painter, L. R. (1974) in *Proceedings of the Advanced Study Institute on Chemical Spectroscopy and Photochemistry in the Vacuum—Ultraviolet* (Sandorfolsy, C., Ansloos, P. J. & Robin, M. B., Eds.) p 129, Reidel, Dordrecht, Holland.

Böttcher, C. J. F., Van Belle, V. C., Bordewij, P., & Rip, A. (1973) *Theory of Electric Polarization*, Vol. 1, Elsevier, Amsterdam.

Bullough, R. K. (1965) *J. Chem. Phys. 43*, 1927–1933.

Caswell, D. S., & Spiro, T. G. (1987) *J. Am. Chem. Soc. 109*, 2796.

Copeland, R. A., & Spiro, T. G. (1985a) *Biochemistry 24*, 1861–1865.

Copeland, R. A., & Spiro, T. G. (1985b) *Biochemistry 24*, 4960–4968.

Copeland, R. A., & Spiro, T. G. (1986) *J. Am. Chem. Soc. 108*, 1281.

Copeland, R. A., & Spiro, T. G. (1987) *Biochemistry 26*, 2134.

Dayhoff, M. O., Hunt, L. T., McLaughline, P. S., & Jones, D. D. (1976) in *Atlas of Protein Sequence and Structure* (Dayhoff, M. O., Ed.) Vol. 5, Suppl. 2, p 208, National Biomedical Research Foundation, Baltimore, MD.

Demchenko, A. P. (1986) *Ultraviolet Spectroscopy of Proteins*, pp 137–144, Springer-Verlag, Berlin, Heidelberg, and New York.

DeVito, V., & Asher, S. A. (1989) *J. Am. Chem. Soc. 111*, 9143–9152.

Dudik, J. M., Johnson, C. R., & Asher, S. A. (1985a) *J. Phys. Chem. 89*, 3805.

Dudik, J. M., Johnson, C. R., & Asher, S. A. (1985b) *J. Chem. Phys. 82*, 1732–1740.

Eckhardt, G., & Wagner, W. G. (1966) *J. Mol. Spectrosc. 19*, 407–411.

Friend, S. H., & Gurd, F. R. N. (1979) *Biochemistry 18*, 4612–4619.

Gilson, M. K., & Honig, B. H. (1986) *Biopolymers 25*, 2097–2119.

Grinspan, H., Birnbaum, J., & Feitelson, J. (1966) *Biochim. Biophys. Acta 126*, 13–18.

Hapner, K. B., Bradshaw, R. A., Hartzell, C. R., & Gurd, F. R. N. (1968) *J. Biol. Chem. 243*, 683.

Harada, I., & Takeuchi, H. (1986) in *Spectroscopy of Biological Systems* (Clark, R. J., & Hester, R. E., Eds.) Chapter 3, John Wiley and Sons, New York.
Harmon, P. A., & Asher, S. A. (1990) *J. Chem. Phys. 93*, 3094–3100.
Harmon, P. A., Teraoka, J., & Asher, S. A. (1990) *J. Am. Chem. Soc. 112*, 8789–8799.
Hermans, J., Jr. (1962) *Biochemistry 1*, 193–197.
Hildebrandt, P. G., Copeland, R. A., Spiro, T. G., Otlewski, J., Laskowski, M., & Prendergast, F. G. (1988) *Biochemistry 27*, 5426.
Hirsch, R. E., & Peisach, J. (1986) *Biochim. Biophys. Acta 872*, 147.
Hudson, B., & Mayne, L. (1984) *Methods Enzymol. 130*, 331.
Johnson, C. R., Ludwig, M., O'Donnell, S., & Asher, S. A. (1984) *J. Am. Chem. Soc. 106*, 5008–5010.
Johnson, C. R., Ludwig, M., & Asher, S. A. (1986) *J. Am. Chem. Soc. 108*, 905–912.
Jones, C. M., DeVito, V. L., Harmon, P. A., & Asher, S. A. (1987) *Appl. Spectrosc. 41*, 1268–1275.
Kaminaka, S., Ogura, T., & Kitagawa, T. (1990) *J. Am. Chem. Soc. 112*, 23–27.
Kirkwood, J. G. (1939) *J. Chem. Phys. 7*, 911–919.
Krimm, S., Song, S., & Asher, S. A. (1989) *J. Am. Chem. Soc. 111*, 4290–4294.
Larkin, P., Gustafson, W., & Asher, S. A. (1990) *J. Chem. Phys. 94*, 5324–5330.
Liu, G., Grygon, C. A., & Spiro, T. G. (1989) *Biochemistry 28*, 5046–5050.
Ludwig, M., & Asher, S. A. (1988a) *J. Am. Chem. Soc. 110*, 1005–1011.
Ludwig, M., & Asher, S. A. (1988b) *Appl. Spectrosc. 42*, 1458–1466.
MacRae, R. A., Williams, M. W., & Arakawa, E. T. (1974) *J. Chem. Phys. 61*, 861.
Mayne, L., & Hudson, B. (1987) *J. Phys. Chem. 91*, 4438.
Mayne, L. C., Zingler, L. D., & Hudson, B. (1985) *J. Phys. Chem. 89*, 3395.
McRae, E. G. (1957) *J. Phys. Chem. 61*, 562–572.
Mirone, P. (1966) *Spectrochim. Acta 22*, 1897–1905.
Myers, A. B., & Mathies, R. A. (1987) in *Biological Applications of Raman Spectrometry* (Spiro, T. G., Ed.) Vol. II, pp 1–58, Wiley, New York.
Nagel, R. L., Ranney, H. M., & Kucinskis, L. L. (1966) *Biochemistry 5*, 1934.
Nestor, J. R., (1972) Ph.D. Thesis, University of Maryland.
Nestor, J. R., & Lippincott, E. R. (1973) *J. Raman Spectrosc. 1*, 305–318.
Onsager, L. (1936) *J. Am. Chem. Soc. 58*, 1486–1493.
Polo, S. R., & Wilson, M. K. (1955) *J. Chem. Phys. 23*, 2376–2377.
Ragone, R., Colonna, G., Balestrieri, C., Servillo, L., & Irace, G. (1984) *Biochemistry 23*, 1871–1875.
Ragone, R., Colonna, G., Bismuto, E., & Irace, G. (1987) *Biochemistry 26*, 2130–2134.
Rava, R. P., & Spiro, T. G. (1984) *J. Am. Chem. Soc. 106*, 4062–4064.
Rava, R. P., & Spiro, T. G. (1985a) *Biochemistry 24*, 1861.
Rava, R. P., & Spiro, T. G. (1985b) *J. Phys. Chem. 89*, 1856.
Rhodes, W. (1961) *J. Am. Chem. Soc. 83*, 3609–3617.
Robinson, L., Birkhoff, R. D., & Arakawa, E. T. (1969) *J. Chem. Phys. 51*, 243–251.
Shire, S. J., Hanania, G. I. H., & Gurd, F. R. N. (1975) *Biochemistry 14*, 1352–1358.
Siamwiza, M. N., Lord, R. C., Chen, M. C., Takamatsu, T., Harada, I., Matsuura, H., & Shimanouchi, T. (1975) *Biochemistry 14*, 4870–4876.
Song, S., & Asher, S. A. (1989) *J. Am. Chem. Soc. 111*, 4295–4305.
Song, S., & Asher, S. A. (1991) *Biochemistry 30*, 1199–1205.
Song, S., Asher, S. A., Krimm, S., & Bandekar, J. (1988) *J. Am. Chem. Soc. 110*, 8547–8548.
Song, S., Asher, S. A., Krimm, S., & Shaw, K. D. (1991) *J. Am. Chem. Soc. 113*, 1155–1163.
Sowers, B. L., Williams, M. W., Hamm, R. N., & Arakawa, E. T. (1972) *J. Chem. Phys. 57*, 167.
Su, C., Park, Y. D., Liu, G. Y., & Spiro, T. G. (1989) *J. Am. Chem. Soc. 111*, 3547–3549.
Sweeney, J. A., & Asher, S. A. (1990) *J. Phys. Chem. 94*, 4784–4791.
Takeuchi, H., Watanabe, N., Satoh, Y., & Harada, I. (1989) *J. Raman Spectrosc. 20*, 233–237.
Teraoka, J., Harmon, P. A., & Asher, S. A. (1990) *J. Am. Chem. Soc. 112*, 2892–2900.
Tinoco, I., Jr. (1960) *J. Am. Chem. Soc. 82*, 4785–4790.
Uyeda, M., & Peisach, J. (1981) *Biochemistry 20*, 2028–2035.
Wilbur, D. J., & Allerhand, A. (1976) *J. Biol. Chem. 251*, 5187–5194.
Williams, E. J. (1966) *Arch. Biochem. Biophys. 115*, 21–26.
Yanari, S., & Bovey, F. A. (1960) *J. Biol. Chem. 235*, 2818–2825.